J. Pharm. Pharmacol. 2000, 52: 263–272
Received September 3, 1999
Accepted October 20, 1999

Design, Synthesis and Evaluation of *N*-Basic Substituted 3-Hydroxypyridin-4-ones: Orally Active Iron Chelators with Lysosomotrophic Potential

ZU D. LIU, HICHAM H. KHODR, SHU L. LU AND ROBERT C. HIDER

Department of Pharmacy, King's College London, Franklin-Wilkins Building, 150 Stamford Street, London SE1 8WA, UK

Abstract

To investigate the possibility of targeting chelators into the lysosomal iron pool, nine bidentate 3-hydroxypyridin-4-ones with basic chains have been synthesized. As the turnover of ferritin iron is centred in the lysosome, such strategy is predicted to increase chelator efficacy of bidentate ligands.

The pK_a values of the ligands together with their distribution coefficients between 1-octanol and 4-morpholinepropane sulphonic acid (MOPS) buffer pH 7·4 have been determined. The in-vivo iron mobilization efficacy of these basic 3-hydroxypyridin-4-ones has been investigated in a ^{59}Fe-ferritin-loaded rat model. No obvious correlation was observed between efficacy and the pK_a value of the side chain, although those with $pK_a > 7{\cdot}0$ tended to be more efficient than those with $pK_a < 7{\cdot}0$. The imidazole-containing molecules are much less effective than the tertiary amine derivatives. A dose–response study suggested that basic pyridinones are relatively more effective at lower doses when compared with *N*-alkyl hydroxypyridinones.

Optimal effects were observed with the piperidine derivatives **4h** and **4i**. The derivative **4i** at a dose of $150\,\mu mol\,kg^{-1}$ was more effective than $450\,\mu mol\,kg^{-1}$ deferiprone, the widely adopted clinical dose.

Frequent blood transfusion remains the basic therapeutic treatment for the survival of β-thalasaemia major patients. Such long-term blood transfusion leads to the accumulation of excess iron and the associated toxic consequences. Complications associated with elevated iron levels can be largely avoided by the use of iron-specific chelating agents and in particular desferrioxamine. Unfortunately, desferrioxamine lacks oral activity and this has a dramatic influence on patient compliance (Hershko et al 1998).

3-Hydroxypyridin-4-ones are one of the main candidates for the development of orally active iron chelating alternatives to desferrioxamine (Tilbrook & Hider 1998). Indeed, the 1,2-dimethyl derivative (deferiprone) is the only orally active iron chelator currently available for clinical use. Unfortunately, the dose required to keep a previously well-chelated patient in negative iron balance appears to be relatively high ($450\,\mu mol\,kg^{-1}$). Not surprisingly therefore, side effects have been observed in some patients receiving deferiprone (Hershko et al 1998).

In order to improve drug efficacy or decrease drug toxicity, it is necessary to design a chelator that can be efficiently and selectively delivered to its site of action such as the liver, the major iron storage organ. The possibility of using an ester prodrug strategy to increase drug absorption and hepatic extraction, thereby increasing the drug efficacy has been previously investigated (Liu et al 1999a; Rai et al 1999). Results demonstrated that selective targeting of a chelator to the liver is possible (Choudhury et al 1997; Liu et al 1999a). This strategy can be further refined by targeting the drug not only to the hepatocyte, but to lysosomes located in the hepatocyte.

Lysosomes are intracellular organelles that contain over 40 hydrolytic enzymes each possessing acid pH optima. The major functions of lysosomes include intracellular digestion, transcellular transport, extracellular release or secretion of their contents, and the sequestration and storage of

Correspondence: R. C. Hider, Department of Pharmacy, King's College London, Franklin-Wilkins Building, 150 Stamford Street, London SE1 8WA, UK.
E-Mail: robert.hider@kcl.ac.uk

endogenous or exogenous cell components (de Duve 1963). As can be seen from the lysosomal catabolism of ferritin (Figure 1), ferritin is constantly broken down in cells within lysosomes and much of the liberated iron is reincorporated into new ferritin molecules (Pippard et al 1986; Radisky & Kaplan 1998). Therefore, it is expected that the acidic lysosomal compartment possesses a relatively high concentration of iron in a chemical form suited to efficient chelation. This conclusion is further endorsed by the results of Laub et al (1985) who, by using radiolabelled desferrioxamine, showed that the likely source of chelatable iron in the hepatocyte is the lysosomal pool. Thus, the selective delivery of chelating agents to lysosomes may greatly improve their efficiency in iron removal from iron overloaded patients.

3-Hydroxypyridin-4-ones with basic side chains might be expected to accumulate in acidic organelles such as lysosomes more efficiently than neutral compounds (de Duve et al 1974). Such a strategy is demonstrated in the two compartment model represented in Figure 2. If it is assumed that only neutral molecules are able to cross lysosomal membranes, then at equilibrium the concentration of the neutral form will be the same in both compartments. Thus, the distribution ratio (DR) can be calculated from equation 1:

$$\begin{aligned}\text{Distribution ratio (DR)} &= [L_{total}]_B/[L_{total}]_A \\ &= [LH]_B(1 + 10^{pKa-pH_B})/ \\ &\quad [LH]_A(1 + 10^{pKa-pH_B}]\end{aligned}$$

$$\text{If } [LH]_B = [LH]_A \text{ then}$$

$$DR = (1 + 10^{pKa-pH_B})/1 + 10^{pKa-pH_A}) \qquad (1)$$

For a compound with a pK_a value of 6·0, over 90% will be neutral at pH 7·0, whereas at pH 5·0 over 90% of the compound will be protonated. Thus the equilibrium accumulation of drug in the acidic intravesicular compartment B (pH 5·0) is calculated as 10. If it is assumed that the drug is maintained at a constant concentration in the cytoplasm (pH 7) (for example 25 μM), then the total drug concentration (neutral form and protonated form) in the acidic lysosomes (pH 5·0) will be 250 μM. Such an elevated lysosomal concentration of chelator would be predicted to increase the chelator efficacy of bidentate ligands.

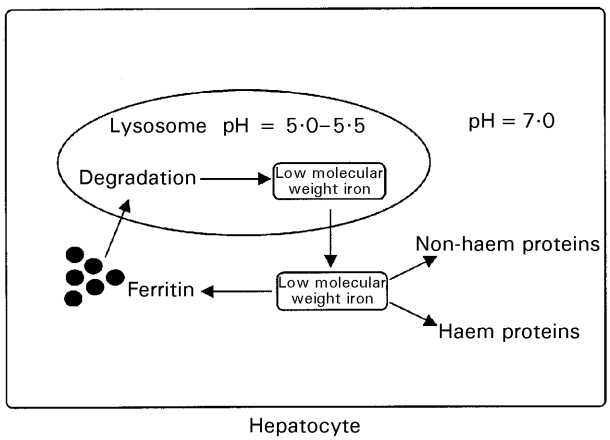

Figure 1. Schematic representation of the major intracellular iron fluxes in the hepatocyte.

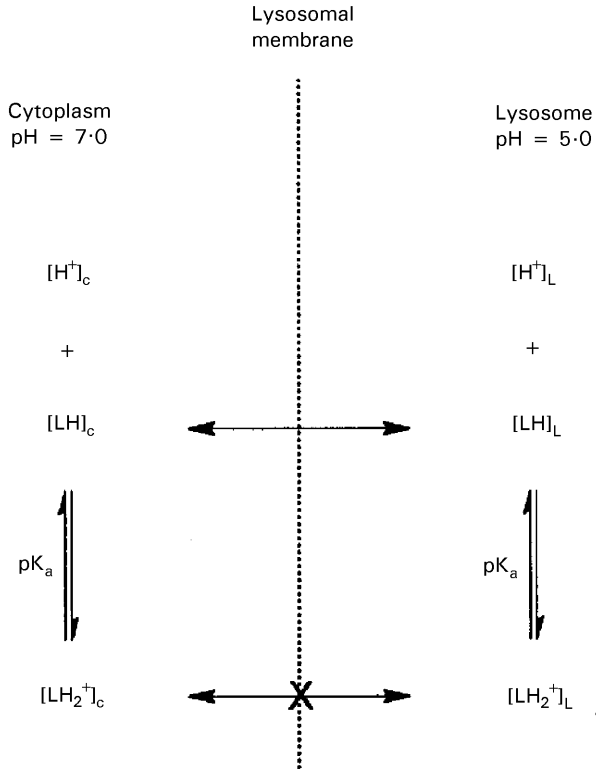

Figure 2. Distribution of a monobasic drug between the cytoplasm (pH 7·0) and the lumen of the lysosome (pH 5·0–5·5).

Normally only the neutral uncharged form can cross biological membranes at an appreciable rate. Therefore, when attempting to design a basic compound with a useful accumulation effect, the proportion of non-ionized species present at pH 7·0 must also be considered since this may greatly influence the penetration rate of such drugs into the cell. The fraction of non-ionized species (Fn) can be calculated from equation 2:

$$\begin{aligned}\text{Neutral fraction } (F_n) &= [LH]/([LH] + [LH_2^+]) \\ &= 1/(1 + 10^{pKa-pH}) \qquad (2)\end{aligned}$$

For compounds with a pK_a value less than 6·0, the fraction of non-ionized species (which can cross the cell membrane) at pH 7·0 is relatively high but the equilibrium distribution ratio is relatively low (Figure 3). In contrast, drugs with pK_a values greater than 8·0 have a greater chance of accumu-

lating efficiently within the cell. However, the penetration rate of such compounds into the cell will be much slower due to the high proportion of ionized species present at pH 7·0 (Figure 3). Ideally, drugs for accumulation in the lysosome should not only possess an appreciable distribution ratio but must also be able to penetrate the cell at a sufficiently high rate. It is predicted that an ideal chelator for this purpose should have a pK_a value in the range of 6·0–8·0, although it has been suggested in the literature that the optimum pK_a value for lysosomotropic agents is around 8 (de Duve et al 1974). Thus, it is expected that chelators possessing such properties would scavenge iron more effectively at lower doses than the corresponding neutral ligands.

In order to achieve the optimum pK_a value (pK_a 6–8) for the lysosomotrophic chelation approach, it is necessary to select suitable basic side chains for hydroxypyridinone ligands. 3-Hydroxypyridin-4-ones have two resonance forms (a and b) and the major resonance form (b) possesses an appreciable positive charge located on the ring nitrogen atom (Figure 4). Due to this positive charge on the nitrogen, the pyridinone ring will exert an electron withdrawing effect on the side chain. Since the net charge on the hydroxypyridinone is less than unity ($\sim 0{\cdot}7^{+}$) (Xiao et al 1992), it is expected that the pyridinone ring will have a somewhat reduced influence on the basic function than, for example, a protonated amino group. Indeed preliminary studies indicate that the basic strength of the 3-hydroxypyridin-4-one side chain is increased compared with the corresponding unsubstituted amine, the pK_a values being approximately 10% greater

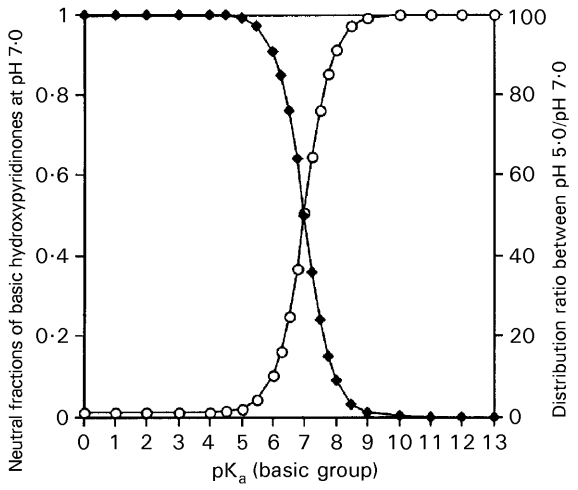

Figure 3. The relationship between pK_a value of a monobasic drug with equilibrium distribution ratio between two compartments (pH 5·0 and pH 7·0) (○), and the noncharged fraction of the drug at pH 7·0 (◆).

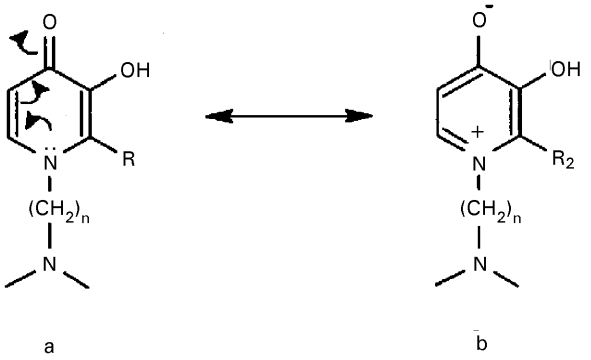

Figure 4. The mesomeric effect of the pyridin-4-one ring. 3-Hydroxypyridin-4-ones have two resonance forms (a and b) and the major resonance form (b) possesses an appreciable positive charge located on the ring nitrogen atom.

(Dehkordi 1996). It is therefore possible to predict the pK_a value of the basic group on hypothetical 3-hydroxypyridin-4-ones if the pK_a values of the corresponding amine are known. Adopting this approach, a range of *N*-basic substituted 3-hydroxypyridin-4-ones have been synthesized by selecting amines such as histamine, 1-(amino-propyl) imidazole, *N*,*N*-dimethyl-ethylenediamine, *N*,*N*-diethylethylenediamine, 1-(2′-aminoethyl)-pyrrolidine and 2-piperidinoethylamine.

Materials and Methods

Chemistry

Maltol and ethyl maltol were purchased from Pfizer Ltd (Widnes, UK). All other chemicals were obtained from Aldrich Chemical Co. (Gillingham, UK). Melting points were determined using an Electrothermal IA 9100 Digital Melting Point Apparatus (Southend, UK) and are uncorrected. ^{1}H NMR spectra were recorded using a Perkin-Elmer (60 MHz) NMR spectrometer (Tokyo, Japan). Chemical shifts (δ) are reported in ppm downfield from the internal standard tetramethylsilane (TMS). Elemental analyses were performed by Micro analytical laboratories, Department of Chemistry, The University of Manchester (Manchester M13 9PL, UK). The synthetic pathway of the basic 3-hydroxypyridin-4-ones is summarized in Figure 5.

*2-Methyl-3-benzyloxypyran-4(1H)-one (**2a**).* Sodium hydroxide (22 g, 0·55 mol, 1·1 eq.) dissolved in water (50 mL) was added to a solution of maltol (**1a**) (63 g, 0·5 mol, 1 eq.) in methanol (500 mL) followed by benzyl chloride (69·6 g, 0·55 mol, 1·1 eq.). The resulting mixture was refluxed for 6 h. After removal of solvent by rotary evaporation, the residue was mixed with water (250 mL) and extracted with dichloromethane (3 × 150 mL). The

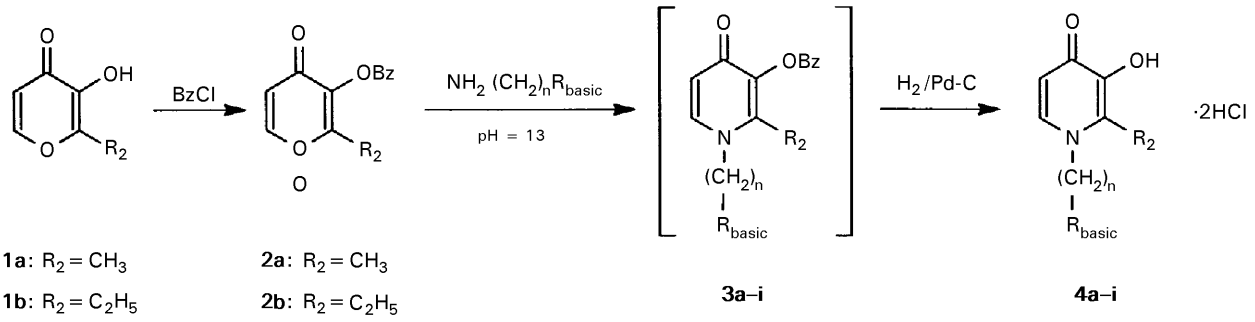

Figure 5. Synthesis of basic 3-hydroxypyridin-4-ones.

combined extracts were washed with 5% aqueous sodium hydroxide (2 × 250 mL) followed by water (2 × 250 mL). The organic fraction was then dried over anhydrous sodium sulphate, filtered and rotary evaporated. This yielded an orange oil which solidified on cooling. Recrystallization from diethyl ether gave the pure product (**2a**) as colourless needles (92·5 g, 85·6%); mp 52–53°C; ^{1}H NMR ($CDCl_3$) δ: 2·10 (s, 3H, 2-*CH*$_3$), 5·10 (s, 2H, *CH*$_2$Ph), 6·3 (d, 1H, 5-*H*(pyranone)), 7·32 (s, 5H, *Ar*), 7·54 (d, 1H, *6-H*(pyranone)).

An analogous procedure using ethyl maltol (**1b**) gave 2-ethyl-3-benzyloxypyran-4(1H)-one (**2b**) (84·8%). mp 33–34°C; ^{1}H NMR ($CDCl_3$) δ: 1·0 (t, 3H, 2-CH$_2$ *CH*$_3$), 2·55 (q, 2H, 2-*CH*$_2$CH$_3$), 5·13 (s, 2H, *CH*$_2$Ph), 6·3 (d, 1H, 5-*H*(pyranone)), 7·35 (s, 5H, *Ar*), 7·6 (d, 1H, *6-H*(pyranone)).

*General method for the preparation of basic 3-hydroxypyridin-4-ones (**4a–i**).* Selected amine (30 mmol, 1·5 eq.) was added to a solution of **2a** or **2b** (20 mmol, 1 eq.) in ethanol (50 mL)/water (50 mL) followed by 2 M sodium hydroxide solution until pH 13·5 was obtained. The mixture was then refluxed for 12 h. After adjustment to pH 1 with conc. hydrochloride acid, the solvent was removed by rotary evaporation before addition of water (50 mL) and washing with diethyl ether (2 × 50 mL). Subsequent adjustment of the aqueous fraction to pH 9 with 10 M sodium hydroxide solution was followed by extraction into dichloromethane (4 × 50 mL). The combined organic layers were then dried over anhydrous sodium sulphate, filtered, and then rotary evaporated to give a brown oil. Purification by column chromatography on silica gel (eluant: 12% CH_3OH/88% $CHCl_3$) gave the benzylated hydroxypyridinones **3a–i** as a yellow oil, which was subsequently dissolved in ethanol (90 mL)/water (10 mL) and subjected to hydrogenolysis in presence of 5% Pd/C (5–10% w/w of the compound) catalyst for 2 h. After filtration, the pH of the solution was adjusted to 1 using conc. hydrochloride acid and the solvent was then removed in-vacuo to yield the crude product. Re-crystallization from methanol/diethyl ether gave the pure compound (**4a–i**) as a white or yellow solid.

*1-[2′-(Imidazol-4-yl)ethyl]-2-methyl-3-hydroxypyridin-4(1H)-one dihydrochloride (**4a**).* Yield 52%; mp 239–240°C; ^{1}H NMR (DMSO-d$_6$) δ: 2·54 (s, 3H, *2-CH*$_3$), 3·2 (t, 2H, NCH$_2$*CH*$_2$), 4·65 (t, 2H, N*CH*$_2$CH$_2$), 7·3 (d, 1H, *5-H*(pyridinone)), 7·44 (s, 1H, *5-H* (imidazole)), 8·18 (d, 1H, *6-H*(pyridinone)), 9·08 (s, 1H, *2-H*(imidazole)). Anal. Calc. for $C_{11}H_{15}N_3O_2Cl_2$: C, 45·21; H, 5·14; N, 14·38%. Found: C, 45·57; H, 5·07; N, 13·98%.

*1-[3′-(Imidazol-1-yl)propyl]-2-methyl-3-hydroxypyridin-4(1H)-one dihydrochloride (**4b**).* Yield 69%; mp 160–161°C;^{1}H NMR (DMSO-d$_6$) δ: 2·2–2·75 (m, 2H, CH$_2$*CH*$_2$CH$_2$), 2·6 (s, 3H, *2-CH*$_3$), 4·1–4·8 (m, 4H, *CH*$_2$CH$_2$*CH*$_2$), 7·4 (d, 1H, *5-H* (pyridinone)), 7·7 (d, 1H, *5-H*(imidazole)), 7·92 (d, 1H, *6-H*(imidazole)), 8·4 (d, 1H, *6-H*(pyridinone)), 9·38 (s, 1H, *2-H*(imidazole)), 6·1–8·8 (br., 3H, OH and NH). Anal. Calc. for $C_{12}H_{17}N_3O_2Cl_2{\cdot}H_2O$: C, 44·46; H, 5·91; N, 12·96%. Found: C, 44·43; H, 5·79; N, 12·72%.

*1-[3′-(Imidazol-1-yl)propyl]-2-ethyl-3-hydroxypyridin-4(1H)-one dihydrochloride (**4c**).* Yield 59%; mp 189–191°C; ^{1}H NMR (DMSO-d$_6$) δ: 1·03 (t, 3H, 2-CH$_2$*CH*$_3$), 1·85–2·55 (m, 2H, CH$_2$*CH*$_2$CH$_2$), 2·8 (q, 2H, 2-*CH*$_2$CH$_3$), 3·9–4·8 (m, 4H, *CH*$_2$CH$_2$*CH*$_2$), 7·4 (d, 1H, *5-H*(pyridinone)), 7·65 (d, 1H, *5-H*(imidazole)), 7·9 (d, 1H, *6-H*-(imidazole)), 8·35 (d, 1H, *6-H*(pyridinone)), 9·35 (s, 1H, *2-H*(imidazole)). Anal. Calc. for

$C_{13}H_{19}N_3O_2Cl_2$: C, 48·76; H, 5·98; N, 13·12%. Found: C, 48·64; H, 5·82; N, 12·94%.

*1-[2′-(Dimethylamino)ethyl]-2-methyl-3-hydroxypyridin-4(1H)-one dihydrochloride (**4d**)*. Yield 65·7%; mp 251–252°C; ^{1}H NMR (D_2O) δ: 2·58 (s, 3H, *2-CH*$_3$), 3·0 (s, 6H, N(*CH*$_3$)$_2$), 3·4–3·9 (m, 2H, N-CH$_2$*CH*$_2$N(CH$_3$)$_2$), 4·75 (t, 2H, N-*CH*$_2$CH$_2$N(CH$_3$)$_2$), 7·1 (d, 1H, *5-H*(pyridinone)), 8·1 (d, 1H, *6-H*(pyridinone)). Anal. Calc. for $C_{10}H_{18}N_2O_2Cl_2$: C, 44·61; H, 6·69; N, 10·41%. Found: C, 44·26; H, 6·85; N, 10·04%.

*1-[2′-(Dimethylamino)ethyl]-2-ethyl-3-hydroxypyridin-4(1H)-one dihydrochloride (**4e**)*. Yield 52%; mp 234–236°C; ^{1}H NMR (D_2O) δ: 1·28 (t, 3H, 2-CH$_2$*CH*$_3$), 2·75–3·3 (q, 2H, 2-*CH*$_2$CH$_3$), 3·05 (s, 6H, N(*CH*$_3$)$_2$), 3·5–3·9 (m, 2H, N-CH$_2$ *CH*$_2$N(CH$_3$)$_2$), 4·74 (t, 2H, N-*CH*$_2$CH$_2$N(CH$_3$)$_2$), 7·15 (d, 1H, *5-H*(pyridinone)), 8·1 (d, 1H, *6-H*(pyridinone)). Anal. Calc. for $C_{11}H_{20}N_2O_2Cl_2{\cdot}H_2O$: C, 43·86; H, 7·36; N, 9·30%. Found: C, 43·73; H, 7·24; N, 9·21%.

*1-[2′-(Diethylamino)ethyl]-2-methyl-3-hydroxypyridin-4(1H)-one dihydrochloride (**4f**)*. Yield 85·5%; mp 244–247°C (dec); ^{1}H NMR (DMSO-d$_6$) δ: 1·26 (t, 6H, N(CH$_2$*CH*$_3$)$_2$), 2·6 (s, 3H, *2-CH*$_3$), 2·9–3·8 (m, 6H, N(*CH*$_2$CH$_3$)$_2$ and N-CH$_2$*CH*$_2$N(C$_2$H$_5$)$_2$), 4·9 (t, 2H, N-*CH*$_2$CH$_2$N(C$_2$H$_5$)$_2$), 7·4 (d, 1H, *5-H*(pyridinone)), 8·45 (d, 1H, *6-H*(pyridinone)), 9·1–10·4 (br., 3H, *OH* and *NH*). Anal. Calc. for $C_{12}H_{22}N_2O_2Cl_2$: C, 48·49; H, 7·46; N, 9·42%. Found: C, 48·29; H, 7·35; N, 9·28%.

*1-[2′-(1-Pyrrolidinyl)ethyl]-2-methyl-3-hydroxypyridin-4(1H)-one dihydrochloride (**4g**)*. Yield 71%; mp 234–236°C;^{1}H NMR (D_2O) δ: 1·9–2·5 (m, br., 4H, - *CH*$_2$*CH*$_2$-(pyrrolidine ring)), 2·64 (s, 3H, *2-CH*$_3$), 2·8–3·8 (m, br., 4H, -*CH*$_2$-N-*CH*$_2$-(pyrrolidine ring)), 3·75 (t, 2H, (pyridinone)N-CH$_2$ *CH*$_2$N(pyrrolidine)), 4·8 (t, 2H, (pyridinone)N-*CH*$_2$CH$_2$N(pyrrolidine)), 7·2 (d, 1H, *5-H*(pyridinone)), 8·21 (d, 1H, *6-H*(pyridinone)). Anal. Calc. for $C_{12}H_{20}N_2O_2Cl_2{\cdot}H_2O$: C, 46·02; H, 7·08; N, 8·94%. Found: C, 46·17; H, 6·82; N, 8·68%.

*1-(2′-Piperidinoethyl)-2-methyl-3-hydroxypyridin-4(1H)-one dihydrochloride (**4h**)*. Yield 75·6%; mp 213–215°C; ^{1}H NMR (D_2O) δ: 1·3–2·4 (m, br., 6H, -*CH*$_2$*CH*$_2$*CH*$_2$-(piperidine ring)), 2·64 (s, 3H, *2-CH*$_3$), 2·7–4·2 (m, 6H, -*CH*$_2$-N-*CH*$_2$-(piperidine ring) and (pyridinone)N-CH$_2$*CH*$_2$N(piperidine)), 4·8 (t, 2H, (pyridinone)N-*CH*$_2$CH$_2$N-(piperidine)), 7·18 (d, 1H, *5-H*(pyridinone)), 8·18 (d, 1H, *6-H*(pyridinone)). Anal. Calc. for $C_{13}H_{22}N_2O_2Cl_2{\cdot}H_2O$: C, 47·71; H, 7·39; N, 8·56%. Found: C, 47·94; H, 7·32; N, 8·42%.

*1-(2′-Piperidinoethyl)-2-ethyl-3-hydroxypyridin-4(1H)-one dihydrochloride (**4i**)*. Yield 65%; mp 207–209°C; ^{1}H NMR (D_2O) δ: 1·22 (t, 3H, 2-CH$_2$ *CH*$_3$), 1·4–2·5 (m, br., 6H, -*CH*$_2$*CH*$_2$*CH*$_2$-(piperidine ring)), 3·0 (q, 2H, 2-*CH*$_2$CH$_3$), 3·1–3·9 (m, 6H, -*CH*$_2$-N-*CH*$_2$-(piperidine ring) and (pyridinone)N-CH$_2$ *CH*$_2$N(piperidine)), 4·8 (t, 2H, (pyridinone)N-*CH*$_2$CH$_2$N (piperidine)), 7·18 (d, 1H, *5-H*(pyridinone)), 8·18 (d, 1H, *6-H*(pyridinone)). Anal. Calc. for $C_{14}H_{24}N_2O_2Cl_2{\cdot}H_2O$: C, 49·27; H, 7·68; N, 8·21%. Found: C, 49·01; H, 7·49; N, 8·04%.

Determination of physicochemical properties of ligands—pK_a determination. Equilibrium constants of protonated ligands were determined using an automated computerized system (Taylor et al 1988). This consisted of a Metrohm 665 dosimat (Herisau, Switzerland), a Perkin-Elmer Lambda 5 UV/vis Spectrophotometer (Beaconsfield, UK), a Corning Delta 225 pH meter, and an IBM compatible PC (Opus Technology, Taiwan) to control the integrated system. A combined Sirius electrode was used to calibrate the electrode zero and to measure pH values. This system is capable of undertaking simultaneous potentiometric and spectrophotometric measurements. A blank titration of 0·1 M KCl (25 mL) was carried out to determine the electrode zero using Gran's plot method (Gran 1952). The solution (0·1 M KCl, 25 mL), contained in a jacketed titration cell, was acidified by 0·15 mL 0·2 M HCl. Titration was carried out against 0·3 mL 0·2 M KOH using 0·01 mL increments dispensed from the dosimat. Solutions were maintained at $25 \pm 0{\cdot}5$°C under an argon atmosphere. The above titration was repeated in the presence of ligand. The data obtained from titration were subjected to non-linear least-square regression analysis using the NONLINM1 program (Taylor et al 1988). The pK_a values were obtained to an accuracy of $\pm 0{\cdot}02$ pH unit.

Determination of distribution coefficients. Distribution coefficients were determined using an automated continuous flow technique (Rai et al 1998). The system comprised an IBM compatible PC running the Omniferous Personal Computer Auto-Titrator "TOPCAT" program, which controlled a Metrohm 665 Dosimat autoburette and a Pye-Unicam Lambda 5 UV/vis spectrophotometer, as well as performing all calculations of distribution coef-

ficients. Determinations were performed using AnalaR grade reagents under a nitrogen atmosphere using a flat-based glass vessel equipped with a sealable lid at 25°C. The aqueous and octanol phases were presaturated with respect to each other before use. The filter probe consisted of a polytetrafluoroethylene plunger associated with a gel-filtration column. The aqueous phase (50 mM MOPS buffer, pH 7·4, prepared using Milli-Q water) was separated from the two-phase system (1-octanol/4-morpholinepropane sulphonic acid (MOPS) buffer, pH 7·4) by means of a hydrophilic cellulose filter 5-μm diameter, 589/3 Blauband filter paper, Schleicher and Schuell) mounted in the gel-filtration column adjuster (SR 25/50, Pharmacia). MOPS was adopted as a buffer for this study because of its low affinity for metal cations. A known volume (normally 25–50 mL) of MOPS buffer (saturated with octanol) is taken in the flat base mixing chamber. After a base line was obtained the solution was used for reference absorbance. The compound to be examined was dissolved in buffer (saturated with octanol) so as to give an absorbance of between 0·5–1·5 absorbance units at the preselected wavelength ($\sim$280 nm). The flow rate of the aqueous circuit was limited to 1 mL. The computer program calculates the distribution coefficient ($D_{7\cdot4}$) for each octanol addition.

Biological experiment

Animals. Male Wistar rats were purchased (local breed) from A. Tuck & Son (Battlesbridge, Essex SS1, UK) and housed in the Biological Service Unit, King's College London. The animals were maintained at 20–23°C, with food and water freely available. All animal experiments performed were specified in project licence PPL 70/4561, authorized by the Secretary of State (England) under Animals Act 1986.

Iron mobilization efficacy study in ^{59}Fe-ferritin-loaded rat. Hepatocytes of normal fasted rats (190–230 g) were labelled with ^{59}Fe by administration of [^{59}Fe]ferritin to the tail vein (Liu et al 1999b). One hour later, each rat was administered orally with chelator. Control rats were administered with an equivalent volume of water. The rats were placed in individual metabolic cages and urine and faeces collected. Rats were allowed access to food 1 h after oral administration of chelator. There was no restriction of water throughout the study period. The investigation was terminated 24 h after the [^{59}Fe]ferritin administration, rats were killed and the liver and gastrointestinal tract (including its content and faeces) were removed for gamma counting. The "iron mobilization" and "efficacy" were calculated according to equations 3 and 4:

$$\text{Iron mobilization (\%)} = (^{59}\text{Fe-activity}_{(\text{gut and faeces})} / (^{59}\text{Fe-activity}_{(\text{gut and faeces})} + ^{59}\text{Fe-activity}_{(\text{liver})})) \times 100\% \quad (3)$$

$$\text{Efficacy (\%)} = \text{iron mobilization (\%)} - \text{control (\%)} \quad (4)$$

Results

Chemistry

The basic 3-hydroxypyridin-4-ones **4a**–**i** were conveniently prepared by utilizing the methodology of Harris and co-workers (Figure 5) (Harris 1976). Commercially available 3-hydroxypyran-4-ones **1a** and **1b** were benzylated in aqueous methanol. The reactions of the protected pyranones (**2a** and **2b**) with an excess of primary amines were generally performed by refluxing in 50% aqueous ethanol in the presence of a catalytic amount of sodium hydroxide. Removal of the protecting benzyl group was achieved by catalytic hydrogenation to yield the corresponding bidentate chelators, which were finally isolated as the hydrochloride salts. Nine substituted 3-hydroxypyridin-4-ones (**4a**–**i**) were prepared by using selected amines (Table 1).

pK_a values of basic hydroxypyridinones

All ligands were investigated by simultaneous spectrophotometric and potentiometric titration. The pH dependence of the UV spectra of **4i** (Figure 6) is presented as an example. A clear shift in λ_{max} was observed in the full speciation spectra of ligand **4i** over pH range 2·05–11·98 (Figure 6) which displays the pH dependence of the ligand ionization equilibrium. The optimized pK_a values obtained from non-linear least-square regression analysis are shown in Table 1. All the basic 3-hydroxypyridin-4-ones in this study possess three pK_a values. The pK_a1 values correspond to the protonation of the 4-oxo group, the pK_a2 values to the deprotonation of the basic function at the 1-position and pK_a3 to the dissociation of the 3-hydroxyl group (Figure 7). The pK_a values obtained from spectrophotometric titration were in good agreement with those calculated from the potentiometric titration (Table 1). The speciation plot of **4i** (Figure 8) provides information on the distribution of the species in the

Table 1. Basic hydroxypyridinones (**4a–i**) and their measured physicochemical properties.

Compound	R_{basic}	n	R_2	pK_a (poteniometric)			pK_a (spectrophotometric)			$D_{7.4}$ (n = 5)	F_n (pH 7·4)	Log P	DR
				pK_{a1}	pK_{a2}	pK_{a3}	pK_{a1}	pK_{a2}	pK_{a3}				
4a	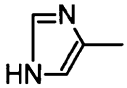	2	CH_3	3·01	6·25	9·80	2·99	6·23	9·81	0·293 ± 0·006	0·935	−0·504	15·7
4b	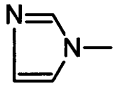	3	CH_3	3·08	6·71	9·82	3·13	6·60	9·92	0·344 ± 0·005	0·848	−0·382	31·8
4c	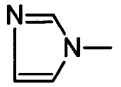	3	C_2H_5	3·15	6·47	9·66	3·09	6·55	9·71	0·420 ± 0·019	0·886	−0·324	25·2
4d	$(CH_3)_2N$	2	CH_3	2·86	7·02	9·58	2·74	7·05	9·75	0·154 ± 0·005	0·699	−0·657	52·5
4e	$(CH_3)_2N$	2	C_2H_5	2·68	7·16	9·58	2·62	6·88	9·66	0·538 ± 0·047	0·706	−0·118	51·6
4f	$(C_2H_5)_2N$	2	CH_3	2·66	7·50	9·60	2·63	7·53	9·65	0·493 ± 0·005	0·434	0·055	76·8
4g	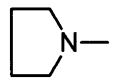	2	CH_3	2·64	7·69	9·61	2·70	7·60	9·61	0·285 ± 0·011	0·363	−0·105	81·7
4h	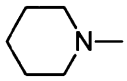	2	CH_3	2·88	7·47	9·71	2·77	7·42	9·63	0·960 ± 0·029	0·474	0·307	73·9
4i	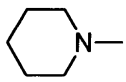	2	C_2H_5	2·74	7·38	9·70	2·73	7·34	9·67	4·591 ± 0·031	0·523	0·943	69·9

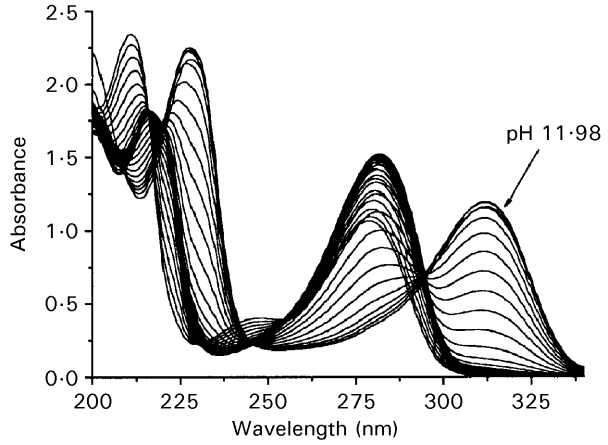

Figure 6. pH dependence of the UV spectrum of **4i** over the pH range 2·05–11·98.

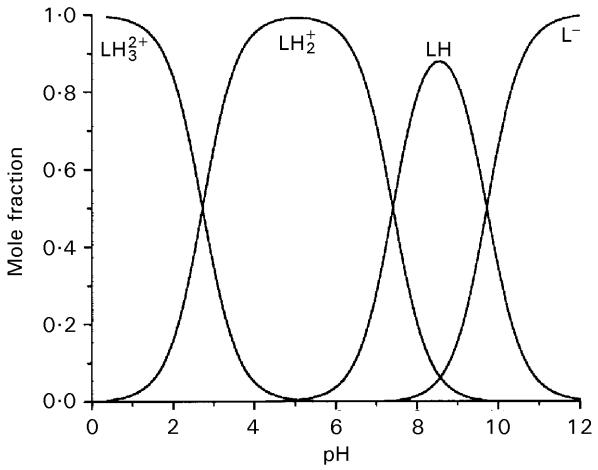

Figure 8. The pH dependence of the speciation plot of **4i**.

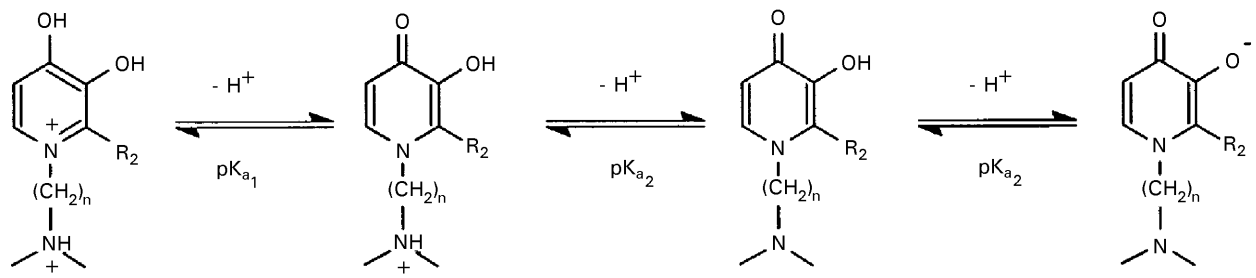

Figure 7. Protonation equilibria of basic 3-hydroxypyridin-4-ones.

pH range of 0–12. Therefore, the predominant species can be predicted at specific pH values.

Distribution and partition coefficients of basic hydroxypyridinones

The distribution coefficients ($D_{7.4}$) between 1-octanol and MOPS buffer (pH 7·4) were determined via the automated filter-probe system. As a result of the degree of ionization of the two functional groups on the pyridinone ring (pK_a1 and pK_a3) being relatively small at pH 7·4, the neutral fraction (F_n) of the basic hydroxypyridinones can be calculated by employing the pK_a2 values determined above. The partition coefficient (P) of each compound can then be calculated from equation 5. The resulting values are given in the Table 1.

$$F_n = 1/(1 + 10^{pKa2 - pH})$$
$$P = D_{7.4}/F_n = D_{7.4} \times (1 + 10^{pKa2 - pH}) \qquad (5)$$

Iron mobilization efficacy of basic hydroxypyridinones

In-vivo iron scavenging ability of basic hydroxypyridinones was compared with deferiprone. Several compounds such as **4e**, **4g**, **4h** and **4i** were found to be superior to deferiprone (Table 2). The imidazole-containing ligands **4a**, **4b** and **4c** were found to be much less effective than the tertiary amine derivatives. The most effective basic hydroxypyridinone was **4i**, which possesses a piperidine substitutent, with an associated efficacy at 450 μmol kg^{-1} of 26·5%. Dose–response experiments have also been undertaken with the following compounds, deferiprone, **4g**, **4h** and **4i** at three different doses (150, 300 and 450 μmol kg^{-1}). All three basic compounds, **4g**, **4h** and **4i**, performed better than deferiprone at low doses. In particular **4i** was more effective at 150 μmol kg^{-1} than deferiprone at 450 μmol kg^{-1}.

Table 2. Iron mobilization efficacy studies of basic hydroxypyridinones (**4a**–**i**) in the [^{59}Fe]ferritin-loaded rat model.

Chelator	Dose (μmol kg^{-1})	Iron mobilization (%)	Efficacy (%)
Control	–	3·9 ± 1·0	0·0
Deferiprone	450	13·4 ± 5·2	9·5
	300	9·2 ± 2·2	5·4
	150	6·3 ± 2·1	2·4
4a	450	5·5 ± 2·5	1·6
4b	450	5·3 ± 1·9	1·4
4c	450	6·8 ± 3·5	2·9
4d	450	13·0 ± 2·5	9·1
4e	450	20·3 ± 6·8	16·4
4f	450	12·4 ± 1·9	8·5
4g	450	18·8 ± 3·6	14·9
	300	13·9 ± 3·5	10·0
	150	9·5 ± 1·8	5·6
4h	450	22·7 ± 3·3	18·8
	300	15·2 ± 1·8	11·3
	150	11·5 ± 1·6	7·6
4i	450	30·4 ± 5·3	26·5
	300	17·9 ± 2·3	14·0
	150	14·2 ± 3·2	10·3

Values are expressed as means ± s.d. (n = 5).

Discussion

To investigate the possibility of achieving lysosomotrophic strategy, a range of bidentate 3-hydroxypyridin-4-ones with basic side chains was synthesized. The compounds fell into two classes, the imidazoles (**4a**–**c**) and tertiary amines (**4d**–**i**). The log P values covered the range −0·12–0·943 (Table 1). Therefore, it was anticipated that all compounds would be orally active and some may well be susceptible to efficient first-pass extraction by the liver. By incorporating selected basic functions into the pyridinone ring, the pK_a values of the basic side chain covered the desired range (6·24–7·64).

In-vivo iron mobilization efficacy of all ligands was evaluated in a non-iron overloaded rat model. [^{59}Fe]Ferritin was used to label the liver iron pool, and this was followed by a challenge with a test chelator at a time when the iron released by lysosomal degradation of ferritin was maximally available (Pippard et al 1981; Liu et al 1999b). This [^{59}Fe]ferritin-loaded rat model can be used to assess oral bioavailability and to compare the ability of chelators to remove iron from liver, the major iron storage organ in iron-overloaded conditions. Several basic hydroxypyridinones led to superior iron excretion via the bile compared with deferiprone (Table 2). There was no obvious correlation between efficacy and the pK_a value of the side chain, although those with $pK_a > 7·0$ tended to be more efficient than those with $pK_a < 7·0$. The imidazole-containing molecules were much less effective than the tertiary amine derivatives. This may result from unfavourable metabolism of the imidazole function. Comparison of the tertiary amino-containing pyridinones highlights **4i** as the most promising candidate. It is likely that **4i** was the most efficient at facilitating the excretion of iron because of its relatively high log P value (0·943) and hence more efficient extraction by the liver.

One of the reasons for investigating basic hydroxypyridinones is the belief that they will be relatively more effective at lower concentrations than neutral hydroxypyridinones due to their

predicted accumulation by hepatocyte lysosomes. Consequently, the dose–response experiment was undertaken in order to investigate the predicted lysosomotrophic effect of basic hydroxypyridinones. Detailed comparisons of efficacy between different doses are made in Table 3. Generally, the efficacy of basic hydroxypyridinones decreased more slowly than that of deferiprone. The efficacy ratios of **4g**, **4h** and **4i** (0·376, 0·404 and 0·387, respectively) were greater than that for deferiprone (0·253) between 150 and 450 μmol kg^{-1}. The largest differences occurred over the more dilute dose range 150–300 μmol kg^{-1}, where the ratios were larger for the basic hydroxypyridinones, particularly **4h** and **4i**.

There are, however, potential disadvantages associated with bidentate iron ligands in therapeutic applications such as kinetic lability, concentration dependence on iron speciation and the possible toxicity of 2 : 1 (ligand : iron) complexes (Tilbrook & Hider 1998). For bidentate 3-hydroxypyridin-4-ones such as **4i**, the 3 : 1 complex was the dominant species at pH 7·0 (Figure 9A), due to the high affinity for iron(III). However, such 3 : 1 complexes tend to dissociate under acidic conditions, for instance those found in lysosomes (pH 5·0–5·5). With a ligand (**4i**) concentration of 1×10^{-5} M ($[Fe^{III}] = 1 \times 10^{-6}$ M) at pH 5·0, the 2 : 1 complex will be the major species (Figure 9A). With the 2 : 1 complexes, the incompletely enveloped iron atom is able to interact with hydrogen peroxide or oxygen to generate free radicals (Tilbrook & Hider 1998). However, if such basic bidentate chelators can be efficiently accumulated in the lysosomal compartments, then the ligand-metal complex will dissociate less readily in the presence of the resulting higher concentration of ligand. Thus any toxicity associated with the presence of $Fe^{III}L_2^+$ species would be reduced. As shown in Figure 9B, at the higher ligand concentration of 7×10^{-4} M, which is the predicted lysosomal concentration of **4i**, the 3 : 1 complex will be the dominant species even at pH 5·0. Under these conditions, the concentration of the 2 : 1 complex is negligible.

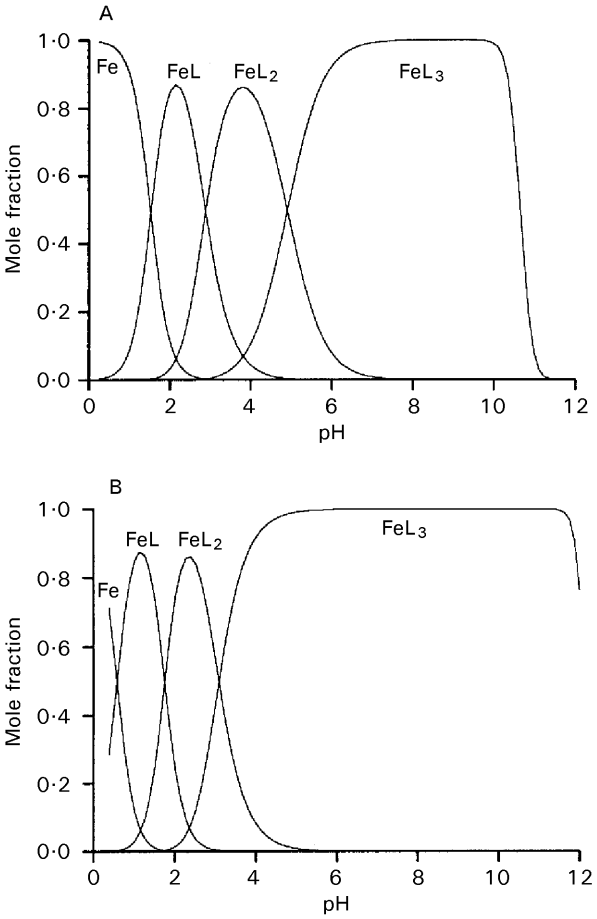

Figure 9. Comparison of the speciation plots of **4i**-iron(III) complex at different ligand concentrations. $[Fe^{III}]_{total} = 1 \times 10^{-6}$ M; A, $[\mathbf{4i}] = 1 \times 10^{-5}$ M; B, $[\mathbf{4i}] = 7 \times 10^{-4}$ M. The following measured parameters were incorporated into the model for the system: $\log\beta_1(ML) = 14{\cdot}40$, $\log\beta_2(ML_2) = 26{\cdot}49$, $\log\beta_3(ML_3) = 36{\cdot}38$, $pK_a1 = 2{\cdot}73$, $pK_a2 = 7{\cdot}34$, $pK_a3 = 9{\cdot}67$.

The precise pH value between the lysosome and the cytoplasm in the hepatocyte is unknown. If the pH of the lysosome is 5·0, then the introduction of one basic group on the molecule can lead to a maximum accumulation of approximately 100

Table 3. Efficacy ratio of hydroxypyridinones between different doses.

Chelator	Efficacy ratio between different doses		
	Efficacy$_{(300\,\mu mol\,kg^{-1})}$/ Efficacy$_{(450\,\mu mol\,kg^{-1})}$	Efficacy$_{(150\,\mu mol\,kg^{-1})}$/ Efficacy$_{(300\,\mu mol\,kg^{-1})}$	Efficacy$_{(150\,\mu mol\,kg^{-1})}$/ Efficacy$_{(450\,\mu mol\,kg^{-1})}$
Deferiprone	0·568	0·444	0·253
4g	0·671	0·560	0·376
4h	0·601	0·673	0·404
4i	0·528	0·736	0·389

between those two phases (Figure 3). If however the intralysosomal pH is 5·5, the maximum accumulation effect drops to 32. In contrast, the introduction of two basic groups leads to a maximum accumulation of 10^4 between two phases differing by 2 pH units and 10^3 for 1·5 pH units. Thus, a more dramatic concentration dependence of efficacy might be predicted for dibasic chelators.

In conclusion, the fundamental concept of basic hydroxypyridinones being relatively more effective at lower doses has been confirmed in this study. Selection of the basic substitutent is critical, a pK_a value $\geqslant 7{\cdot}0$ being necessary to provide enhanced iron scavenging ability. To improve the efficacy of this chelator class, it will be necessary to design monobasic and dibasic molecules that experience efficient liver extraction.

Acknowledgements

The research described in this manuscript was supported by Apotex Research Inc. Canada and Biomed EC grant BMH4-CT97-2149. Z. D. Liu would like to thank the KC Wong Education Foundation (Hong Kong) and the Committee of Vice-Chancellors and Principals of the Universities of the United Kingdom for the joint scholarships that enabled him to carry out the studies.

References

Choudhury, R., Epemolu, R. O., Rai, B. L., Hider, R. C., Singh, S. (1997) Metabolism and pharmacokinetics of 1-(2′-trimethylacetoxyethyl)-2-ethyl-3-hydroxypyridin-4-one (CP117) in the rat. Drug Metab. Dispos. 25: 332–339

de Duve, C. (1963) The lysosome concept. In: de Reuck, A. V. A., Cameron, M. P. (eds) Lysosomes, a CIBA Foundation Symposium, Boston, pp 1–35

de Duve, C., de Barsy, T., Poole, B., Trouet, A., Tulkens, P., van Hoof, F. (1974) Lysosomotropic agents. Biochem. Pharmacol. 23: 2495–2531

Dehkordi, L. S. (1996) Design Of Orally Active Pyridinone Iron(III) Selective Ligands. Ph.D. Thesis. King's College London

Gran, G. (1952) Determination of the equivalence point in potentiometric titration. Analyst 77: 661–671

Harris, R. L. N. (1976) Potential wool growth inhibitors. Improved synthesis of mimosine and related 4(1H)-pyridones. Aust. J. Chem. 29: 1329–1334

Hershko, C., Konijn, A. M., Link, G. (1998) Iron chelators for thalasaemia. Br. J. Haematol. 101: 399–406

Laub, R., Schneider, Y. J., Octave, J. N., Trouet, A., Crichton, R. R. (1985) Cellular pharmacology of desferrioxamine B. Biochem. Pharmacol. 34: 1175–1182

Liu, Z. D., Liu, D. Y., Lu, S. L., Hider, R. C. (1999a) Synthesis, physicochemical properties and biological evaluation of aromatic ester prodrugs of 1-(2′-hydroxyethyl)-2-ethyl-3-hydroxypyridin-4-one (CP102): orally active iron chelators with clinical potential. J. Pharm. Pharmacol. 51: 555–564

Liu, Z. D., Lu, S. L., Hider, R. C. (1999b) In vivo iron mobilisation evaluation of hydroxypyridinones in ^{59}Fe-ferritin loaded rat model. Biochem. Pharmacol. 57: 559–566

Pippard, M. J., Johnson, D. K., Finch, C. A. (1981) A rapid assay for evaluation of iron chelating agents in rats. Blood 58: 685–692

Pippard, M. J., Tikerpae, J., Peters, T. J. (1986) Ferritin iron metabolism in the rat liver. Br. J. Haematol. 64: 839

Radisky, D. C., Kaplan, J. (1998) Iron in cytosolic ferritin can be recycled through lysosomal degradation in human fibroblasts. Biochem. J. 336: 201–205

Rai, B. L., Dekhordi, L. S., Khodr, H., Jin, Y., Liu, Z., Hider, R. C. (1998) Synthesis, physicochemical properties and evaluation of N-substituted-2-alkyl-3-hydroxy-4(1H)-pyridinones. J. Med. Chem. 41: 3347–3359

Rai, B. L., Liu, Z. D., Liu, D. Y., Lu, S. L., Hider, R. C. (1999) Synthesis, physicochemical properties and biological evaluation of ester prodrugs of 3-hydroxypyridin-4-ones: design of orally active chelators with clinical potential. Eur. J. Med. Chem. 34: 475–485

Taylor, P. D., Morrison, I. E. G., Hider, R. C. (1988) Microcomputer application of nonlinear regression analysis to metal-ligand equilibria. Talanta 35: 507–512

Tilbrook, G. S., Hider, R. C. (1998) Iron chelators for clinical use.In: Sigel, A., Sigel, H. (eds) Metal Irons in Biological Systems. Vol. 35: Iron Transport and Storage in Microorganisms, Plants and Animals. Marcel Dekker, New York, pp 691–730

Xiao, G., van der Helm, D., Hider, R. C., Dobbin, P. S. (1992) Structure-stability relationships of 3-hydroxypyridin-4-one complexes. J. Chem. Soc. Dalton Trans. 3265–3271